

Neural Network Based Satellite Tracking For Deep Space Applications

Farid Amoozegar, Charles Ruggier

*Jet Propulsion Laboratory
California Institute Of Technology
4800 Oak Grove Drive
Mail Stop 161-260
Pasadena, California, 91109*
Farid.Amoozegar@jpl.nasa.gov
(818) 354-7428
Charles.J.Ruggier@jpl.nasa.gov
(818) 354-1823

ABSTRACT

NASA has been considering the use of Ka-band for deep space missions primarily for downlink telemetry applications. At such high frequencies, although the link will be expected to improve by a factor of four, the current Deep Space Network (DSN) antennas and transmitters would become less efficient due to higher equipment noise figures and antenna surface errors. Furthermore, the weather effect at Ka-band frequencies will dominate the degradations in link performance and tracking accuracy. At the lower frequencies, such as X-band, conventional CONSCAN or Monopulse tracking techniques can be used without much complexity, however, when utilizing Ka-band frequencies, the tracking of a spacecraft in deep space presents additional challenges. The objective of this paper is to provide a survey of neural network trends as applied to the tracking of spacecrafts in deep space at Ka-band under various weather conditions, and examine the trade-off between tracking accuracy and communication link performance.

1. INTRODUCTION

NASA's Deep Space Network (DSN) has been using 34m, and 70m diameter antennas to track and communicate with the spacecrafts, primarily at X-band frequencies. The principal motivation for operating in the Ka-band frequencies is the 4 MHz channel bandwidth limitation at X-band with maximum of 50 MHz spectrum allocation for deep space applications. As the spectrum for X-band becomes more congested, efforts are being made to utilize the Ka-band, which is 3.8 times higher in frequency than X-band (DSN). Ka-band provides 3.8^2 (14.5 times) more Equivalent Isotropic Radiated Power (EIRP) for the same spacecraft transmitter power and antenna size. This provides 5 to 10 dB improvement in signal strength for a given spacecraft transmitter and antenna. The effectiveness of Ka-band operation can be reduced by atmospheric induced noise, pointing loss, scintillation, and fading.

On the commercial side of the space applications, the motive for Ka-band operation is derived from its potential for global communications in the gigabit range. As an example,

inspired by the Asynchronous Transfer Mode (ATM) era technology, suit-case size science terminals have been developed for broadband two-way satellite links. Ka-band operations for near Earth applications also enables the integration of GPS and cellular wireless technology, and leads to further development of the Ka-band for deep space applications.

One real example of Ka-band operation for deep space missions is the NASA Mars Reconnaissance Orbiter (MRO) with telemetry data rates of 0.5 Mbps to 4.0 Mbps, depending on the Earth-Mars distance. Other future missions can demand 10-100 Mbps and require ten times more spectrum than is available at X-band. After more than two decades, many key Ka-band RF components have been developed, such as high power transmitters (e.g., 35-100 Watts), and low noise amplifiers with low noise figures. However, new challenges remain for Ka-band link optimization applications utilizing more robust antenna tracking methods for varying weather conditions.

In the sections below, the tracking methods for deep space applications with weather effects in the Ka-band will be discussed as follows: First, the tracking methods used for deep space applications will be reviewed in section 2 with a discussion on optimization issues between the communications link performance and tracking accuracy. Sections 3 and 4 cover the effect of weather and the weather forecasting methods developed in recent years using neural networks. Section 5 presents discussions and review from recently published literature for potential uses of neural networks for deep space tracking at Ka-band frequencies.

2. LARGE ANTENNA TRACKING METHODS

DSN antenna diameter sizes range from 9 meters for small antennas, to 34 and 70 meters for the larger tracking antennas. Additional burdens are placed on large Ka-band DSN antennas when tracking low power signals from spacecraft at the extremely large distances involved in typical deep space missions. Aside from gravity deformations, thermal effects, wind disturbances, and mechanical vibrations that impact the antenna performance, the degradation effects of weather also need to be taken into account when assessing link performance. Signal fluctuations and fade depths experienced during tracking caused by weather conditions, can be accurately modeled from the predicted weather statistics. The space-to-Earth round-trip delays and the extremely low signal levels involved introduce other challenges for optimizing the link performance and the antenna tracking accuracy.

2.1 Antenna Pointing

Earth-Orbiting satellites can be tracked using open-loop or closed-loop antenna beam pointing methods. Both methods present advantages and disadvantages to the tracking techniques and one method may be chosen from the other depending on the application. Pointing accuracies are dependent on the ground antenna mechanical distortions, tracked

spacecraft dynamics, frequency band in use, and tropospheric instabilities caused by weather conditions, such as gusty winds. Open-loop tracking, or more commonly called “blind pointing,” functions based on the continuously updated predicted pointing coordinates of the object being tracked. This tracking method is sensitive to environmental conditions, such as wind disturbances and is employed in situations of non-critical tracking, or when wind gusts are within certain pointing accuracy tolerance levels. Blind pointing is sometimes preferred over closed-loop pointing during certain experiments that require operator control of the tracked object.

Closed-loop method relies on the initial predicted pointing coordinates of the tracked object, and then continuously corrects the antenna off-beam errors using the amplitude and/or phase components of the signal received from the tracked spacecraft. In contrast to the open-loop method, this method is less sensitive to weather conditions and effectively “tracks out” a significant portion of the pointing error sources encountered during tracking.

2.2 Closed-loop Tracking

Closed-loop tracking is generally superior to open-loop tracking due mainly to its responsiveness to antenna mechanically induced noise, which degrades the pointing accuracy. The antenna pointing error is largely affected by the mechanical jitter caused by wind gusts and other mechanical vibrations to the antenna structure. These random error sources are known to severely degrade the antenna tracking accuracy in the Ka-band, where the antenna beamwidth is effectively narrower and hence more sensitive to angular displacements. Instantaneous antenna pointing errors caused by variations in the atmosphere significantly impact the overall tracking accuracy and to some extent can be tracked out with closed-loop tracking.

2.2.1 CONSCAN Tracking Method

The closed-loop CONSCAN tracking technique has been successfully used to track spacecrafts at the NASA DSN stations. Angle tracking is accomplished by scanning the antenna around its boresight in a circular pattern with constant angular offset, called the scan radius. This technique uses fluctuation of the Automatic Gain Control (AGC) samples from the ground receiver to estimate the ground antenna pointing angle [1]. The circular pattern is chosen such that the received power is 0.1 dB less than the peak power at the antenna boresight. Typically, the 0.1 dB power loss corresponds to 22 mdeg at S-band, 5.9 mdeg at X-band, and 1.5 mdeg at Ka-band (31.8 GHz to 32.3 GHz).

Using the CONSCAN technique, the antenna is rotated at a constant rate ω in a circular pattern about a point called the CONSCAN center. The known instantaneous location of the antenna boresight is defined by X_{ai} given by [2]

$$X_{ai} = \begin{bmatrix} R \cos(\omega t_i) \\ R \sin(\omega t_i) \end{bmatrix} \quad (1)$$

where, R is the CONSCAN radius and ω is the CONSCAN frequency. The carrier power P_{ci} can be approximated by [3]

$$P_{ci} = P_{oi} \left(1 - \mu \frac{\beta_i^2}{h^2}\right) + \eta_i \quad (2)$$

where, P_{oi} is the peak power received when the antenna is pointed directly at the target, and h is the antenna half power beam width, $\mu = 4 \ln(2)$, and β_i is the offset angle between the antenna boresight and the target, and η_i is the signal noise. The offset angle β_i is given by

$$\beta_i = \sqrt{(x_i - x_{ai})^T (x_i - x_{ai})} \quad (3)$$

which yields

$$P_{ci}(x_i) = P_{oi} \left[1 - \frac{\mu}{h^2} (x_i - x_{ai})^T (x_i - x_{ai})\right] + \eta_i \quad (4)$$

After combining equations 1 & 2 we obtain,

$$\beta^2 = x_i^T x_i - 2 x_{ai}^T x_i + R^2 \quad (5)$$

which results in the following final form for the received power,

$$P_i(x_i) = P_o \left[1 - \frac{\mu}{h^2} (x_i^T x_i - 2 x_{ai}^T x_i + R^2)\right] + \eta_i \quad (6)$$

Angular pointing error relationships in the CONSCAN elevation (EL) and cross-elevation (XEL) coordinates are shown in figure 1. The antenna boresight describes a circular pattern around the target with radius R . As the antenna scans the pattern, fluctuations in the received power enables target location estimates during the period of the scan cycle. In equation 6, it is assumed that the spacecraft power and location are fixed during the scan cycle. The spacecraft location is then estimated using the least squares solution to determine location \mathbf{x} for the selected CONSCAN scan cycle and scan radius. In the CONSCAN tracking system, fluctuations in the signal amplitude are compared to the mean power to determine target location, whereas other closed-loop tracking systems require knowledge of both the signal amplitude and phase. The monopulse tracking technique employed by various tracking systems utilize both signal amplitude and phase information to estimate more precise pointing coordinates.

2.2.2 CONSCAN Pointing Errors

The CONSCAN steady state closed-loop variance for the elevation and cross-elevation coordinates are given as

$$\sigma_x^2 = \left[\frac{G \sigma_R^2}{(2-G)(KR)^2} \right] \quad (7)$$

$$\sigma_e^2 = \left[\frac{G \sigma_I^2}{(2-G)(KR)^2} \right]$$

Where, σ_R^2 and σ_I^2 are the real and imaginary components of the open loop variance, G is the loop gain, and K is the loop constant.

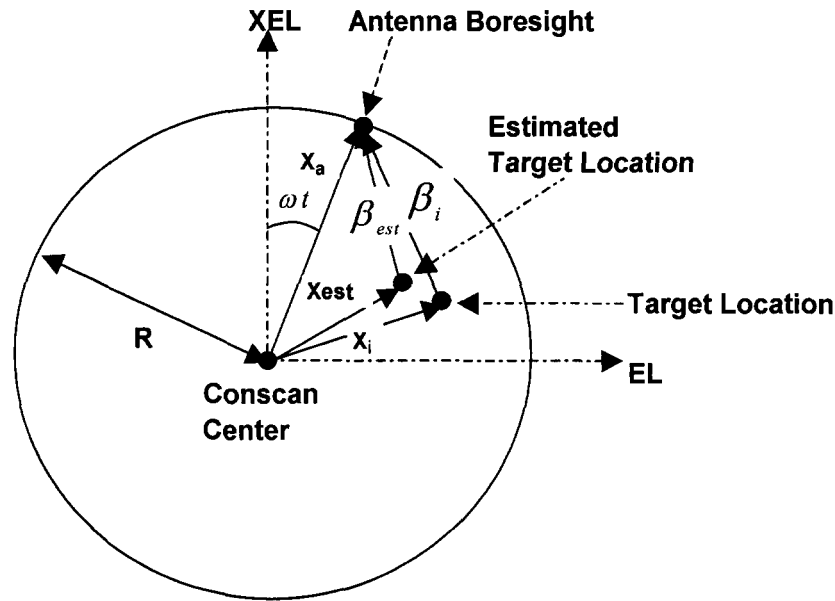


Fig. 1 CONSCAN Geometry

2.2.3 Monopulse Tracking Method

Another closed-loop technique used for tracking spacecraft involves monopulse antenna pointing principles. Monopulse tracking originated with radar monopulse systems that transmit pulses to a tracked target and then receive and process the returned sum and difference signals to determine the angular displacements, or pointing errors. Some monopulse systems employ antennas with multiple feeds and antenna beams to extract the signal amplitude and phase relationships needed for correcting the pointing errors, whereas others employ single multi-mode feeds.

2.2.3.1 Monopulse Tracking System Using Single Multi-Mode Feed

The Ka-band monopulse system employed at the NASA DSN receiver uses a single horn and feed/coupler that separates the sum and difference channels produced by the angular displacements of the antenna beam during tracking. The sum channel consists of the main antenna beam signal, where the gain $G(\theta, \phi)$ peaks at the center of the antenna boresight at $\theta_F = 0$ degrees, as shown in figure 2. Alternately, the antenna error beam pattern consists of a difference, or error signal, which has a gain null at the antenna boresight. The sum channel and the error channel are then compared to yield a tracking error signal.

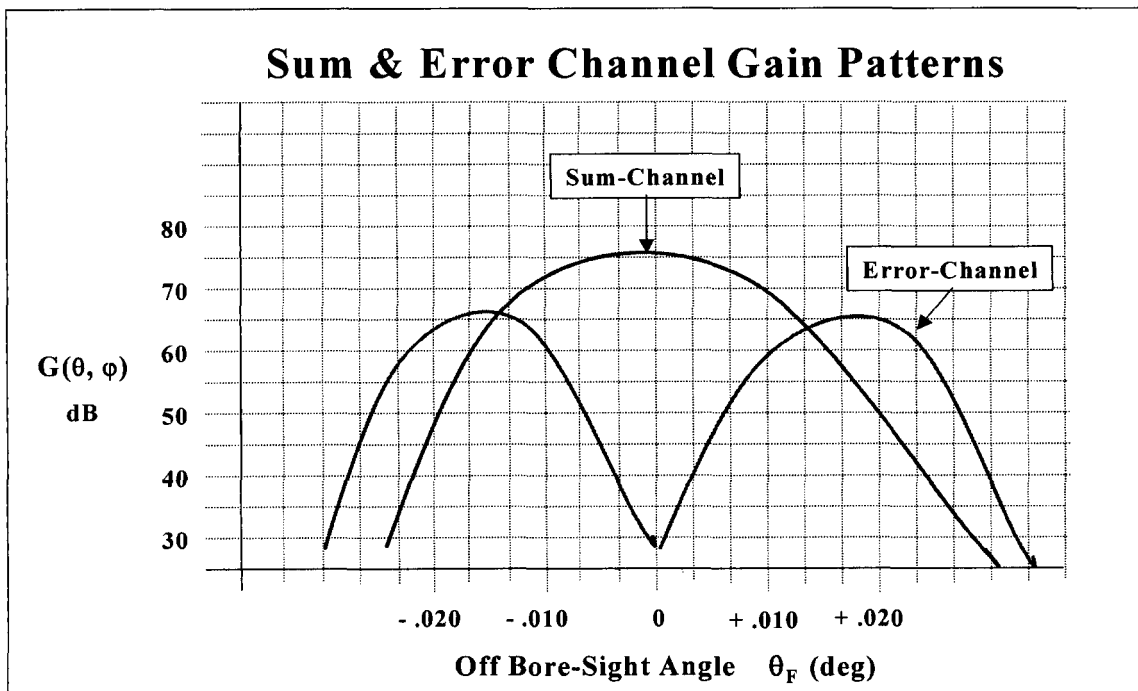


Fig. 2 Monopulse antenna sum & error gain patterns

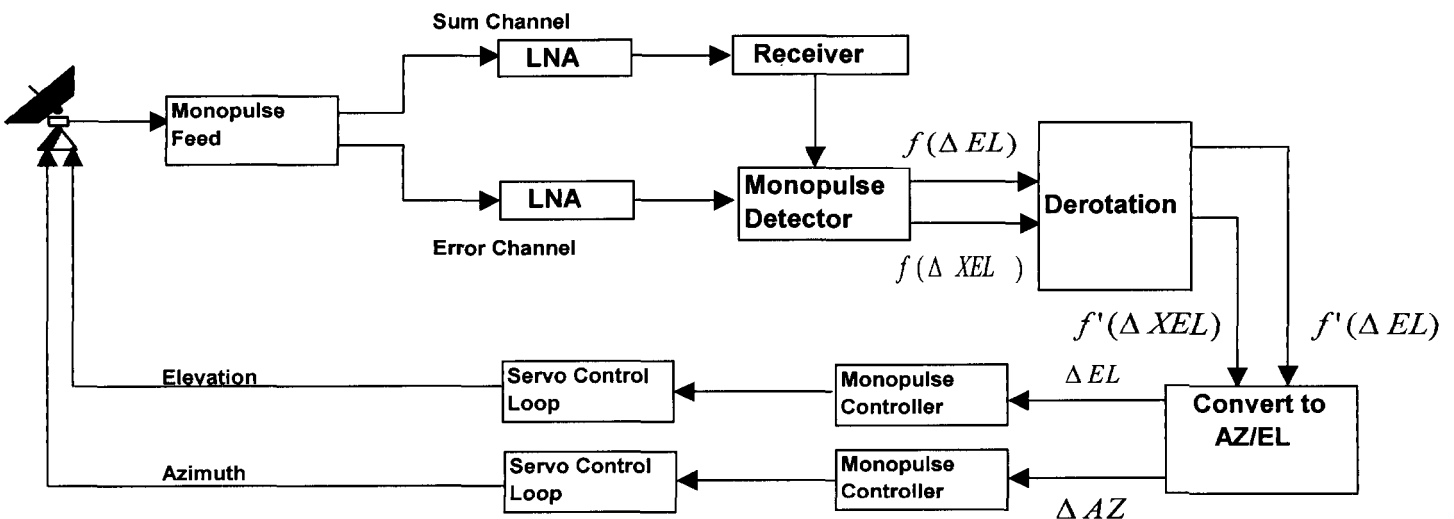


Fig. 3 Monopulse Tracking Loop

Figure 3 shows the sum and error channel monopulse loop configuration. The error channel difference pattern is generated in the antenna feed using waveguide TE₂₁ propagation mode, while the sum channel TE₁₁ dominant mode carries the communications data [4,5]. The amplitude of the received signal at the higher TE₂₁ mode is proportional to the angle of misalignment to the tracked spacecraft. Error signal amplitude and phase components are then detected and processed to drive the antenna servo system, which continuously updates the azimuth and elevation coordinates. The sum and error channels are described as follows,

$$X_s = (2 P)^{1/2} \text{Cos}[\omega_c t + \theta_c + \Delta d(t)] + n_s(t) \quad (8)$$

$$X_e = (2 P)^{1/2} (g(\theta_F, \phi_F))^{1/2} \text{Cos}[\omega_c t + \theta_c + \Delta d(t) + h(\theta_F, \phi_F)] + n_e(t) \quad (9)$$

where,

P = received signal power

$\omega_c t$ = carrier frequency of the received signal

θ_c = phase of the received signal

Δ = modulation index

$d(t)$ = data modulated on the carrier

θ_F = azimuth angle of signal at the feed in a spherical coordinate system
referenced to the feed

ϕ_F = elevation angle of signal at the feed in a spherical coordinate system
referenced to the feed

$(g(\theta_F, \phi_F))^{1/2}$ = ratio of the error signal amplitude and the sum signal
amplitude as a function of (θ_F, ϕ_F)

$h(\theta_F, \phi_F)$ = sum and error channel phase difference in spherical coordinate system
referenced to the feed

$n_s(t)$ = additive white noise in the sum channel

$n_e(t)$ = additive white noise in the error channel

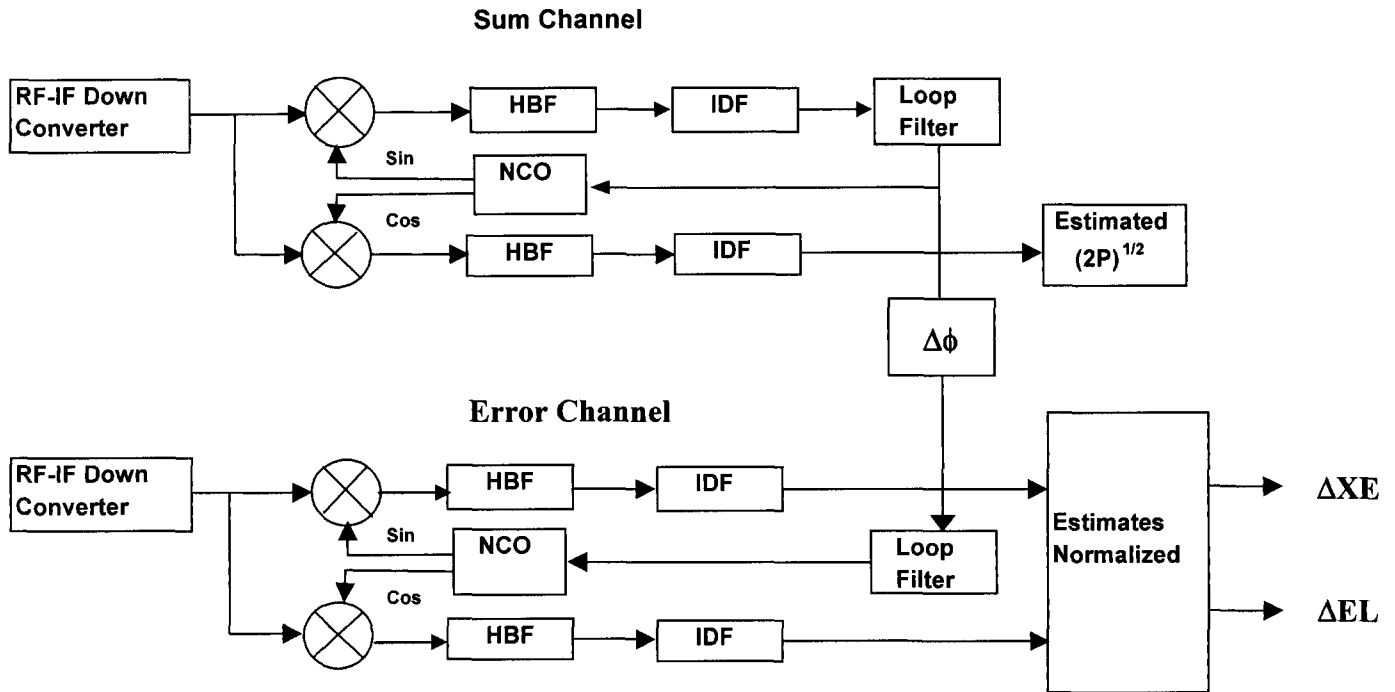


Fig. 4 Monopulse Signal Detection & Processing

A typical monopulse closed-loop system is shown in figure 4. The RF signal is separated into sum and error channel signal at the monopulse feed and amplified independently before being down-converted to IF frequencies. Estimates of the elevation and cross-elevation coordinates are then routed to the multiplier detector stage. Here the sum and error signals are detected as Sine and Cosine components, and passed through a Half-Band Filter (HBF) that couples to an Integrate and Dump Filter (IDF) and the loop filter. An estimate of the relative phase distortion introduced by independent amplification, down conversion and routing is coupled to the error channel loop filter as $\Delta\phi$. The detected sum and error signals are then processed into elevation and cross-elevation coordinates. The monopulse tracking Loop SNR in a 1 Hz loop bandwidth can be estimated as:

$$\text{Tracking Loop SNR} = \frac{P_{c,s}}{N_{0,e} + N_d} \quad (10)$$

Or equivalently,

$$= \frac{P_T}{N_{0,e}} \frac{\text{Cos}^2(m)}{\left(1 + \frac{2 P_T \text{Sin}^2(m)}{N_{0,e} R_s}\right)} \quad (11)$$

where,

$P_{c,s}$ \equiv carrier power in the sum channel

$N_{0,e}$ \equiv one-sided noise power density in the error channel

N_d \equiv equivalent one-sided telemetry data power noise density (i.e., sum channel)

$\frac{P_T}{N_{0,e}}$ \equiv total power-to-noise power density in the error channel

m \equiv telemetry data modulation index

R_s \equiv telemetry symbol rate

The numerator in the second term represents the carrier suppression caused by the telemetry data, and the denominator of the second term represents the additional degradation caused by the noise-like telemetry data power in the loop. It should be noted that with an increase in the symbol rate R_s , there is a corresponding increase in the monopulse tracking loop SNR.

Note again that this is a simple model, and it is assumed that the telemetry data modulation has an equivalent single-sided spectral density similar to the system noise and that its power density can be treated as a white Gaussian noise process, when there is no weather effect.

2.3 Blind Pointing

Antenna “blind pointing” is an open-loop tracking technique based on pointing algorithms determined from the computed positions of the tracked object. Pointing errors are classified as errors in the computed position of the target, and errors due to the differences between the computed target position and the antenna boresight. Systematic and random pointing errors are mainly caused by antenna mechanical jitter, gravitationally induced structural deformities, and atmospheric fluctuations. In most cases, thermal effects will result in pointing errors, which vary slowly with time and require constant self-calibration by the tracking system.

Blind pointing can be used to establish the initial antenna pointing coordinates at the start of a tracking period. This method of open-loop pointing can sometimes be preferred over closed-loop methods, for instances where the pointing error data are used for purposes of experiments. Blind pointing may also be used to track objects that require continuous manual tracking without need for automated tracking control, as when tracking non-radiating objects.

Errors in blind pointing are primarily caused by wind-induced structural deformations. Wind gusts present severe limitations in blind pointing accuracy, especially at the higher frequency bands with narrower antenna beamwidths. Although identifiable systematic error sources in blind pointing can be reduced to manageable levels with the use of various structural metrology devices, random errors are more difficult to control. Alternately, closed-loop tracking systems, such as monopulse tracking, exhibit improved robustness and overall precision in the antenna tracking capability.

2.4 Broadband Monopulse Tracking

In typical cases, the signal received at the monopulse antenna is embedded in noise and has a low signal-to-noise ratio. At the detector, the sum and error sinusoidal signals are routed to phase-locked loops to track and detect the antenna pointing error components. When the received signal power is constant, the signal-to-noise ratio of the monopulse tracking loop can be improved by narrowing the bandwidth of the phase-locked loops. As the signal-to-noise ratio increases there is a corresponding improvement in the pointing error variance.

In the case where the received signal is a broadband type signal, it becomes impracticable to track the signal using narrowband phase-locked loop detection. The tracked broadband noise-like signals are assumed to consist largely of a random noise component and a weak embedded signal with some deterministic structure. Correlation methods provide a more practical approach to detect the amplitude and phase of noise-embedded signals. Broadband monopulse tracking is required when the object being tracked emits a wide spectrum of signals. For example, broadband monopulse tracking may be applied to tracking of quasars or other celestial objects that emit noise-like broadband radio signals.

At the antenna monopulse feed/coupler, the broadband noise-like signal is separated into the TE_{11} and TE_{21} waveguide propagation modes in a manner similar to that of a monochromatic signal. The elevation and cross-elevation pointing errors are detected by cross-correlating and auto-correlating the sum and error channel signals to extract amplitude, phase, and calibration information needed for updating the monopulse loop.

Another application of broadband monopulse tracking is for tracking suppressed carrier signals, such as in the case of BPSK or QPSK modulation, where the carrier is fully suppressed, and the entire signal power is spread out over the frequency band. The tracking system now determines the antenna pointing error from the amplitude and phase information obtained from the modulated signal. For cases when the signal is modulated with random data, such as in telemetry, the spectral characteristics are comparable to broadband noise. The sum and error channel components of this type of signal can be detected using the standard correlation methods described above.

3. WEATHER EFFECTS

Weather is considered to be a major uncontrollable variable of link performance in the Ka-band operation. Links affected by weather require careful analysis of the communications and tracking operating parameters. Examples of operating parameters that can be used to optimize link performance include the modulation index, level of carrier suppression, data rate, carrier power to noise power density in the error channel of tracking loop, receiver lock stability, and tracking accuracy. The weather also affects the method to be used for tracking. Therefore, in order to fully utilize the capabilities of the Ka-band link, adequate and accurate data related to the DSN site atmospheric noise temperature and its corresponding statistics must be collected and analyzed prior to any

link prediction. Furthermore, the development of an optimized link strategy should be coordinated with the tracking method and the corresponding operating parameters. More specifically, for each antenna gain-to-system noise temperature ratio (G/T) prediction, a set of telemetry and tracking parameters need to be selected and set prior to the scheduled tracking period, and refined later if short-term weather prediction becomes available.

To give some examples, 0.3 dB atmospheric loss requires 3 dB link margin, i.e., 0.3 dB atmospheric loss adds 18.36 K to the vacuum 37 K noise temperature. As another example, 1.0 dB atmospheric loss results in 5.02 dB degradation of G/T, which is greater than the typical 3 dB link margin. As a rule-of-thumb, the attenuation of 0-1 dB raises the system noise temperature from 0-60 K linearly. The weather effect further complicates the situation with signal fading, with time durations of 10 seconds to several minutes. On the other hand scintillation at 30 GHz can cause 1 dB variation in carrier-to-noise ratio (CNR).

The link margin improvement of Ka-band over X-band is 11 dB, but with losses as high as 5 dB due to pointing error, 4-10 dB due to bad weather, and 3-10 dB (if not compensated) caused by gravity deformation of the antenna structure, and about 1-2 dB due to wet antenna surface. Therefore, it would be preferable to adopt some weather mitigation technique that is coordinated with the antenna pointing strategy. Typically, 8 mdeg pointing accuracy requirement for X-band corresponds to 2 mdeg of pointing accuracy requirement for Ka-band. Depending on the situation and the availability of X-band and Ka-band sub-systems on-board the spacecraft, a coarse X-band tracking in bad weather could be followed by more precise tracking at Ka-band.

A decision mechanism is needed to act upon the recognized pattern of the weather and relate the telemetry and tracking performance parameters accordingly. The potential of neural network for weather forecast strategies and estimating atmospheric noise temperature as well as local weather patterns are discussed in the following section.

4. NEURAL NETWORK & WEATHER FORECAST

As discussed in the previous section, the most critical and the most uncontrollable factor in Ka-band operation for deep space applications is the effect of weather on tracking and link performance. With regard to weather forecast for various applications, neural networks have been extensively addressed in the literature for numerical weather predictions. Young Yee et al. [7] investigated the use of a neural network in the retrieval of upper level winds and temperature profiles and its effect on the accuracy of ballistic trajectories. Young et al. showed how a neural network could be used for fusion of various meteorology measurements. It was demonstrated how a neural network can be used to estimate the upper level winds from lower level wind measurements. The trained neural net is then used for timely and accurate estimates of the upper level wind effect from calculations of ballistic trajectories.

In another published study, Perez et al. [8] have shown how a trained neural network is able to predict local wind speeds 20 minutes in advance from meteorological sensor inputs, such as wind speed, wind gust, wind direction, air temperature, relative humidity, air pressure, visibility, sunshine duration, net atmospheric radiation, rainfall, solar radiation, and water temperature. A time window was used for the inputs as they are applied to the neural network in a PC. The input features are computed based on the parametric and non-parametric correlation functions.

Pasini et al. [9], involved with neural meteorological forecasting at the Italian Meteorological Service, described the neural research activities for meteorological forecasting such as fog visibility, and forecast of the mean monthly or daily atmospheric temperatures at the site location. Also, in a related work on neural networks, Devendra Singh et al. [10] utilized the High Resolution Picture Transmission (HRPT) reception system installed at the India Meteorological Department to receive real time data from sensors onboard the NOAA-K, L, M, and N series of satellites, and then used neural network methods to retrieve the temperature profiles.

The other aspect of weather forecast mechanism is the prediction of the global surface temperature variations from the greenhouse gases (GHG). For example, A. Walter et al. [11], used a backpropagation neural network (BPN) to take the GHG, the Sulfate aerosol particles (SUA), volcanism (gas-to-particle-conversion), and solar activity, as inputs at each sample time, and output the temperature time series as a response. Yuie-AN Liou et al. [12], used a neural network scheme to generate the surface temperature profile from land and air radiometric relationships, taking into account the atmospheric liquid water and its relation to the surface rain rate.

References [13-15] discussed how neural network can be used to estimate the cloud liquid water content and its contribution to atmospheric noise temperature and rain rate. Neural networks were used to classify the cloud type according to their liquid water content and attenuation effect. Further references are provided for the interested reader for neural network applications of other aspects of weather predictions, such as precipitation, brightness temperature, wind power and speed, classification of local weather patterns, and rain cell top altitude estimation, etc. [15-26].

Therefore, neural networks provide an attractive tool kit for parallel processing of multiple atmospheric parameters that have nonlinear relationships and are difficult to model into joint probability density functions. A neural network can provide a useful interface between the antenna tracking and receiver telemetry. The next section will address the possible trades between tracking and telemetry performance with regard to monopulse tracking, and the potential deployment of neural network for deep space tracking.

5. SATELLITE TRACKING & NEURAL NETWORK FORECASTING

Although the antenna pointing and communications link performance are somewhat correlated, the relationship is nonlinear and the performance parameters can be improved to achieve some level of desired optimization. For instance, monopulse tracking uses the detected signal amplitude and phase components to continually estimate the antenna azimuth and elevation coordinates. The received signal from the spacecraft usually contains telemetry, which is phase-modulated onto the carrier. The telemetry modulation index can be adjusted upward to increase the data E_b/N_0 , or adjusted downward to increase the tracking system P_c/N_0 .

The contributors to tracking errors include receiver noise, servo system noise, target fluctuation (glint noise), atmospheric noise, and signal fading due to weather effects. For the Ka-band operation where atmospheric and weather effects dominate the link performance, the assumption of additive white Gaussian noise is no longer applicable. Effectively, tracking a spacecraft signal in deep space with long (several minutes) round-trip light time becomes equivalent to tracking a conventional fading target. Observing the statistical behavior of weather and the monopulse sum and error signals, we can utilize a neural network to desensitize the effects of fading on the tracking performance.

Monopulse tracking performance has been investigated with regard to the effect of wind and the minimal CNR requirement for tracking in deep space and modeled as a Gaussian random variable at the antenna controller [27]. However, wind constitutes a single component of the entire weather effect, which is more critical at Ka-band. As a specific example of the weather effect, the fading is a higher-level error that needs to be compensated by the tracking system. To improve the tracking performance the weather forecast can be incorporated into the tracking error model. If the CNR required for each class of weather is matched with the receiver loop bandwidth, then the tracking and telemetry performance can be jointly optimized for the effects of weather. This is where a trained neural network can be useful as an interface between the telemetry and tracking systems.

Tracking systems that use neural networks have been discussed in the literature for over a decade. A complete survey of tracking algorithms for aerospace applications using neural network architectures is provided in the references [28]. The advantage of using a neural network between the antenna receiver and tracker is that many subjective behaviors of the antenna through operator experience with weather can be integrated with forecast algorithms and numerical predictions to further improve tracking performance. One example is the recognition of the cloud type and its correlation with atmospheric noise temperature, and deciding on the best data rate, or modulation index to maintain receiver lock while minimizing the tracking error.

V.Y. LO [6] developed monopulse tracking simulation software for the Ka-band 34m Beam Waveguide (BWG) antenna using simulation models. V.Y. LO combined the digital receiver and decoder model with the monopulse antenna pointing model to

evaluate the integrated telemetry and tracking system performance. However, the analysis was limited to wind loading effects on the telemetry and tracking systems.

To date, there have been no known investigations into integrated performance of telemetry and tracking for deep space Ka-band operation under various weather conditions and link characteristics. Data return volume and link optimization methods without regard to tracking system have been formerly investigated [29]. In efforts to improve the large DSN antenna tracking performance, several researchers have utilized neural network techniques. For instance, Vilmotter, and Mukai et al. [30, 31] utilized a Radial Basis Function (RBF) neural network for the DSN 70m fine tracking in the Ka-band downlink. The fine-tracking neural network-based algorithm was obtained from a power-centroid algorithm derived from coarse antenna pointing offsets. Here the neural network was trained to compensate for the gravity distortion, elevation-dependent tracking errors, wind effect, and thermal distortion in such a way as to maximize the signal-to-noise ratio (SNR) of the received signal. The inputs to the neural network in [30] are generated from the seven-array feed elements and combined through the trained neural network, maximizing receiver SNR.

D. Watola and J. B. Hampshire [32] had previously examined the use of a neural network for the Downlink Analyzer (DLA), which was used in the Mars Observer Ka-band Link Experiment. Watola and Hampshire used a neural network with inputs from several weather related sensor read-outs, telecom system parameters, antenna angles, and provided two outputs from the neural network to monitor the data received from the deep space downlink. More specifically, the input parameters included, maximum system noise temperature, azimuth and elevation angles as well as their corresponding error ranges, wind speed, wind speed range, wind direction range, relative wind direction, air temperature, and water vapor density. The neural network was then used to detect and diagnose the data anomalies due to weather, without trying to correct for any tracking, or telemetry parameters.

Therefore, neural networks have the potential for including the impact of the natural phenomena of weather and other environmental effects on the telemetry channel and tracking loops for systems using large antennas. Further details of a neural network algorithm for improved tracking under weather effects will be discussed in a future paper.

CONCLUSION

Neural networks and their applications to space communications and tracking systems affected by weather were discussed. It was shown that neural networks would provide a practical means to optimize telemetry and tracking performance in the Ka-band, which is generally more susceptible to the effects of weather. More in-depth studies are needed to fully characterize the relationships between weather and the tracking and telemetry performance. New efforts are now underway for determining methods for optimizing the telemetry link performance while maintaining the tracking error below the required threshold.

REFERENCES

1. A. Mileant and T. Peng, "Pointing a Ground Antenna at a Spinning Spacecraft Using Conscan-Simulation Results," TDA Progress Report 42-95, Jet Propulsion Laboratory, Pasadena, California, July-September 1988.
2. D. B. Eldred, "An Improved Conscan Algorithm Based on Kalman Filter," TDA Progress Report 42-116, Jet Propulsion Laboratory, Pasadena, California, February 15, 1994.
2. L. Alvarez, "Open Loop Conscan Pointing Error Estimation Accuracy at Ka-band," JPL Interoffice Memorandum 3328-93-044 (internal document), Jet Propulsion Laboratory, Pasadena California, July 8, 1993.
4. M. A. Gudim, W. Gawronski, W. J. Hurd, P. R. Brown, and D. M. Strain, "Design and Performance of the Monopulse Pointing System of the DSN 34-Meter Beam - Waveguide Antennas," TMO Progress Report 42-138, Jet Propulsion Laboratory, Pasadena, California, August 15, 1999.
5. Y. H. Choung, K. R. Goudey, and L. G. Bryans, "Theory and Design of a Ku-Band TE_{21} - Mode Coupler," IEEE Transactions on Microwave Theory and Techniques, Vol. 30, No. 11, November 1982.
6. V. Y. LO, "Ka-band Monopulse Antenna-Pointing Systems Analysis and Simulation", TDA progress report 42-124, Jet Propulsion Laboratory, February 15, 1996.
7. Young Yee et al. "Neural Network Retrieval of Upper Level Winds From Ground-Based Profiler Measurements", US Army Research Laboratory, White Sand Missile Range, NM
8. Perez Liera et al. "Local Short-Term Prediction of Wind Speed: A Neural Network Analysis", Department of Information, University of Oviedo, Gijon, Spain
9. Antonello Pasini et al., "Research in Neural Meteorological Forecasting at the Italian Met Service", perspectives of application to data of a remote telescope site, <http://www.pd.astro.it/TNG/publications/news/16/16itav.html>
10. Devendra Singh et al. "Validation of Atmospheric Temperature Profiles Derived Using Neural Network Approach From AMSU-A Measurements Onboard NOAA-15 and NOAA-16 satellites and Their Applications For Tropical Cyclone Analysis", Satellite Meteorology Division, India Meteorological Department, New Dehli-1003 INDIA
11. A. Walter, M. Denhard and C. D. Schonwiese, "Simulation of global temperature variations and signal detection studies using neural networks", Meteorologische Zeitschrift, N.F.7, pp. 171-180, August 1998.
12. Yuei-AN Liou et al., "The Use of Neural Networks in Radiometric Studies of Land Surface Parameters", Proceedings of National Science Council, Vol. 23, No. 4, pp. 511-517, 1999.
13. Projects at the Radio Communications Research Unit (RCRU), "Slant Path Attenuation at EHF Caused by Cloud", Rutherford Appleton Laboratory
14. Richard L. Bankert, "Cloud Classification of VHRR Imagery in Maritime Regions Using Probabilistic Neural Network", Journal of Applied Meteorology, Vol. 33, pp 909-917, Aug. 1994.

15. E. Moreau et al., "Atmospheric Liquid Water Retrieval Using a Gated Experts Neural Network", American Meteorology Society, April 2002.
16. Bjorn Wiberg and Johan Kjellberg, "Artificial Neural Networks in Weather Prediction", <http://user.it.uu.se/~bjwi7937/kurser/an/projekt/weather.pdf>, project report 2001-06-05,
17. Naoya Maeda et al. "Prediction of Precipitation by A Neural Network Method", Journal of Natural Disaster Science, Vol. 23, NO. 1, pp. 23-33, 2001.
18. Jenni L. Evans and Ana P. Barros, "Satellite tracking and Rainfall Estimation For Short-Term, Heavily Precipitating Storm Events Over Regions of Complex Terrain", The Pennsylvania State University, Land Surface Hydrology Program, NRA 97-MTPE-12.
19. F. Buffa and I. Porceddu, "Temperature forecast and dome seeing minimization", A&A Supplement Series, Vol. 126, pp. 547-553 December 2, 1997.
20. Kiyotaka Miyagishi et al. "Temperature Prediction From Regional Spectral By Neurofuzzy GMDH", Department of Industrial Engineering, College of Engineering, Osaka Prefecture University, 1-1, Gakuencho, Sakai, Osaka, 599-8531, Japan, http://www2.ie.osakafuu.ac.jp/gyouseki/1999/manuscript/99rsm_apiems/99rsm_apiems.pdf
21. V. Montandon et al. "An Hyper-Fast High Spectral Resolution Neural Network-Based Forward Model For The Radiances Observed By The Spatial Interferometer IASI", "Geophysical Research Abstracts, Vol. 5, 11799, 2003.
22. Mituharu Hayashi and Bahman Kermanshahi, "Application of Neural Network For Wind Speed Prediction and Determination of Wind Power Generation Output", Tokio University of Agriculture and Technology, <http://www.tuat.ac.jp/~bahman/achivment/ICEE2001mituharu.pdf>
23. Imran Maqsood et al. "Neurocomputing Based Canadian Weather Analysis", Second International Workshop on Intelligent Systems Design and Applications, Atlanta, USA, August 2002.
24. J.M. Driesse and W.F.S. Poehlman, "Recognizing Local Weather Patterns With Traditional and Neural Network Methods", Department of Engineering Physics, McMaster University, <http://citeseer.nj.nec.com/382988.html>
25. Lj. R. Cander "Neural Networks in Ionospheric Weather Research", CLRC Rutherford Appleton Laboratory, Chilton, Didcot, Oxon OX11 0QX, Great Britain.
26. Michelle S. Spina et al. "Application of Multilayer Feedforward Neural Networks to Precipitation Cell-Top Altitude Estimation", IEEE Transactions on Geoscience and Remote Sensing, Vol. 36, NO. 1, January 1998.
27. W. Gawronski, "Three Models of Wind-Gust Disturbances for the Analysis of Antenna Pointing Accuracy", IPN progress report 142-149, Jet Propulsion Laboratory, May 15, 2002.
28. R. Ghamasae, Farid Amoozegar et al. "Survey of Neural Network as Applied To Target Tracking", Proceedings of SPIE International Conference on Automatic Target Recognition, Volume 3069, April 1997.
29. Shervin Shambayati, "Maximization of Data Return at X-band and Ka-band on the DSN's 34-Meter Beam-Waveguide Antennas", IPN Progress report 42-148, Jet Propulsion Laboratory, February, 2002.

30. V. Vlnrotter and D. Fort, “ Demonstration and Evaluation Of The Ka-band Array Feed Compensation System On The 70-Meter Antenna at DSS 14”, TMO progress report 42-139, Jet propulsion Laboratory, November 15, 1999.
31. Mukai, V. Vlnrotter, and Arabshahi, “ Tracking Performance of Adaptive Array Feed Algorithms For 70-Meter DSN Antennas”, TMO progress report 42-143, Jet Propulsion Laboratory, November 15, 2000.
32. D. Watola, J. B. Hampshire II, “ Automated Downlink Analysis For The Deep Space Network”, TDA progress report 42-126, Jet Propulsion Laboratory, August, 1996.